Keeping the shape but changing the charges: A simulation study of urea and its iso-steric analogs

Jerry Tsai,[a] Mark Gerstein,[b] and Michael Levitt[c]
Program in Biophysics, Department of Structural Biology, Fairchild Building D109, Stanford University, Stanford, California 94305-5400

(Received 28 September 1995; accepted 13 March 1996)

As a first step in simulating solvent denaturation, we compare two possible potentials for urea; one based directly on a parameterization for proteins and another generated from *ab initio*, quantum calculations. Our results, which are derived from numerous, 1 ns simulations, indicate that both potentials reproduce essentially the same observed water structure (as evident in radial distribution functions). However, even though the quantum potential better approximates dimer energies, it is unable to simulate the dynamic behavior of water (as evident in measurements of diffusion) as well as the potential based on protein parameters. To understand its behavior in aqueous solution, we compare the urea simulations with those of solute molecules that possess the same planar, Y-shape as urea but are progressively more hydrophobic. We find that adding urea to a solution increases the number of hydrogen bonds, while adding any of the Y-shaped analogs decreases the number of hydrogen bonds. Moreover, in contrast to the Y-shaped analogs, which aggregate more as they become less polar, we find that urea mixes well in solution and has little tendency to aggregate. For our analysis of aggregation, we used a novel approach based on Voronoi polyhedra as well as the traditional method of radial distribution functions. In conclusion, we discuss how urea's unique behavior in comparison to its Y-shaped analogs has clear implications for models of urea solvation and mechanisms of urea protein denaturation. © *1996 American Institute of Physics.* [S0021-9606(96)50923-2]

I. INTRODUCTION

Over 25 years ago, R. H. Stokes noted that the ''properties of aqueous urea are probably better known than those of any other aqueous nonelectrolyte.''[1] One of the most interesting physical properties that urea imparts to aqueous solutions is the ability to denature proteins.[2,3] Understanding how a polar molecule like urea affects the stability of proteins has motivated many studies of its behavior in solution. In particular, a series of experiments have attempted to discover the mechanism of solvent denaturation by showing that urea increases the solubility of certain hydrophobic molecules[4,5] and of other molecules that mimic the peptide backbone.[6,7] Nozaki and Tanford[8] showed that urea enhances the solubilities of most amino acids with hydrophobic or amide-containing side chains. Building upon these results, Roseman and Jencks[9] found that while hydrophobic molecules are more soluble in other organic cosolvents such as formamide and ethanol, polar molecules containing amide groups are more soluble in aqueous urea.

Two models have been developed to describe urea's aqueous properties. The first was initially proposed by Schellman;[10] furthered by Kreschek and Scheraga;[11] and finally extended by Stokes.[1] (Appropriately, it is named the SKSS model.) These authors attributed urea's aqueous properties to its ability to form dimers and oligomers via hydrogen bonds and measured this interaction by calculating a concentration-independent enthalpy of formation. This model did not consider the other possible interactions in the solution: namely, urea–water and water–water. In contrast, Frank and Franks[12] developed a formalism that involved water's structure (the FF model). They assumed that liquid water exists in an equilibrium between two states; open or ordered vs dense or disordered, and that urea can only dissolve in the disordered state. By interacting only with the disordered state, urea pulls water away from the more ordered state. In this way, urea indirectly ''breaks'' water structure. Although the two models date from the sixties, both explain the thermodynamic data and are useful for interpreting this paper's results.

More recent experimental findings have been mixed, not favoring either model clearly. A NMR study[13] found evidence that urea disturbs long-range water order, and although the authors did not find any stable urea dimers, they did suggest that dimers would occur with lifetimes on the order of picoseconds. Also, a Raman spectroscopy experiment[14] could not find urea dimers in solution. Likewise, other x-ray,[15] fluorometric,[16,17] and calorimetric[18,19] experiments supported the FF model. However, an experiment measuring dielectric relaxation[20] reported very little difference between pure water and a solution with urea; neutron diffraction analysis of urea solutions[21,22] showed that urea does not change water structure appreciably; and one osmotic pressure experiment[23] demonstrated the existence of urea oligomers in solution.

Searching for a more definitive understanding of urea's

[a]Corresponding author. Electronic mail: jotter@hyper.stanford.edu
[b]Electronic mail: mbg@hyper.stanford.edu
[c]Electronic mail: levitt@hyper.stanford.edu

aqueous behavior, investigators have begun to use molecular dynamics in their studies. From their two simulations of ~18 ps each, Tanaka *et al.*[24,25] showed that urea has a negligible effect on water structure and is capable of self-association. Similarly, in their 10 ps study of 1 urea and 210 water molecules, Kuharski and Rossky[26] found no significant disturbance of water structure. At the same time, they analyzed a ternary system of a Lennard-Jones sphere, 200 waters, and one urea placed at the hydrophobic interface for 10 ps and calculated that the single urea was able to displace about three water molecules from the solvation shell of the Lennard-Jones sphere, albeit with some distortion to the water structure at the interface.[27] Lately, studies have concentrated on investigating the stability of the urea dimer. Cristinziano *et al.*[28] modeled a dimer and 40 waters in a truncated octahedron. Their simulation showed the dimer breaking after only 55 ps. Boek and Briels[29] found that urea dimers were even less stable, and suggested that the stability seen by Cristinziano *et al.* was an artifact of their octahedral system. Boek and Briels also reported little disruption of water structure in their 50 ps simulations. On the other hand, Hernández-Cobos *et al.*[30] did find urea dimers in their Monte Carlo simulations of four different urea concentrations, but again saw little disturbance of water structure. Åstrand *et al.* developed a polarizable, *ab initio* potential for urea[31] and conducted four separate simulations of 10 ureas and 277 waters lasting up to 88 ps.[32] They found that urea forms stable dimers and that urea did not significantly affect water structure. Most recently, a Monte Carlo study of urea and *N*-methylacetamide homo and heterodimers again found urea aggregates in solution.[33]

Altogether, both the experimental and simulation evidence do not definitively prove one model over the other.

With the present study, we hope to extend the current understanding of aqueous urea solutions begun by earlier work. We analyze a large number of 1 ns simulations of aqueous urea solutions, which vary in concentration from 0.23 to 6.71 M. Our trajectories are about an order of magnitude longer than formerly reported runs. This is important because very long simulations are necessary to ensure that we properly sample solution space. The simulations of Åstrand *et al.*,[32] the most comprehensive of previous work, sampled only a couple hundred picoseconds. From their study, Åstrand *et al.* noted that their trajectories might not have reached equilibrium since they found urea dimers that were stable for the entire length of the simulation. For reasons discussed later, we believe that their simulations may have been at equilibrium, but that their short trajectories did not sample solution space well enough.

To understand how urea affects aqueous solutions, we compared our urea simulations with similar ones of iso-steric molecules possessing the same, planar Y-shape as urea but differing in polarity. (For a description of the molecules and their charges, see Fig. 1.) We have also run simulations using a more polar, *ab initio* charge set for urea. For simplicity, we refer to this *ab initio* charge distribution as the ''quantum charge set,'' in contrast to the ''simple charge set'' used for the initial series of urea simulations. This quantum charge set was motivated by previous simulation work,[25,30,32] which suggested that the correct modeling of urea's dimer potential would favor formation of complexes in solution. These previous simulations accurately represented the electrostatic interactions inherent in an *ab initio* charge distribution by including higher order terms, such as dipole–quadrupole interactions.[34] Our simulations, in contrast, applied an empirical potential function for electrostatics, which contains only a simple $1/r$ term.[35] Using an *ab initio* charge distribution with our empirical potential is in a sense inappropriate since we do not employ higher order terms in our potential. However, since one objective of these simulations is to find an appropriate parameterization for urea to use with our ENCAD potential, the quantum charge set is useful as a comparison to our simple charge set.

Because all these simulations occur in an aqueous environment, the accuracy of the F3C water model that we used has great influence on our results. Consequently, in Fig. 1 we show the dipole moment and dimer potential for water and also representative interaction energies between water and each solute. The F3C parameterization of water has been shown to reproduce the experimental dynamic, structural, and thermodynamic properties of water quite well, and also to expedite simulations of both protein and DNA.[35–41] Thus, a central goal of this study is to develop a parameterization for urea that is consistent with the previous water and protein simulations for use in future simulations of protein unfolding.

II. METHODS

We used the program ENCAD (Energy Calculation and Dynamics) for all simulations. The program and potentials have been described previously.[35,36] For consistency, parameters for the solutes were based on previously derived values used in protein simulations, except for the urea quantum charge set. In addition, the simulations used all-atom models which included explicit hydrogens. Atoms were allowed all degrees of freedom; however, the solutes containing an sp^2-hybridized, central carbon atom, such as urea, were restrained to a planar configuration using an improper torsion angle term. This model does not completely restrict hydrogen atoms from bending out of plane. Like Åstrand *et al.*,[42] we chose this less than rigid model as a balance between results from Meier and Coussens[43] gas phase, quantum calculation, which showed that urea's hydrogens may be slightly out of plane in vacuum, and other quantum calculations on formamide–water systems,[44–46] which suggested that water stabilizes a planar configuration. Solute molecules were placed in a standard box of 216 waters. All waters closer than 1.67 Å to the nonhydrogen atoms of the solute were removed. Then, the box was scaled to the appropriate volume V_{box} using the solution's experimental[47,48] density $\rho(\mathrm{M})$ at molarity M using

$$V_{\mathrm{box}}=\frac{m_{\mathrm{box}}}{\rho(M)}\times\frac{V_w}{m_w},$$

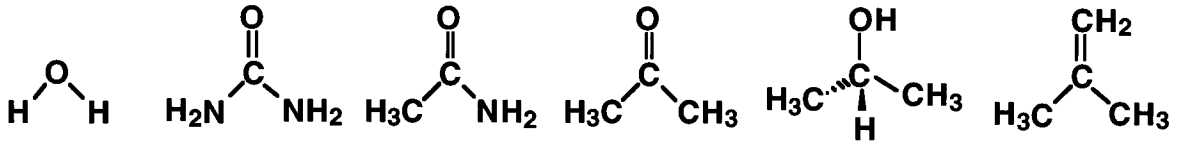

	Water	Urea		Acetamide	Acetone	Isopropanol	Isobutylene
		simple	quantum†				
dipole @	2.5	4.0	5.1	3.6	2.9	2.1	0.2
dimer ¥	-7.2	-8.3	-16.3				
w/ water#	--	-7.7	-12.0	-7.3	-5.9	-5.0	-2.9

Charge Distributions[a]

O	-0.820	O	-0.740	-0.380	O	-0.380	O	-0.380	H	0.433	$H_{(2)}$	0.119
$H_{(2)}$	0.410	C	1.280	0.380	C	0.380	C	0.380	O	-0.433	C	-0.238
		N	-1.170	-0.666	N	-0.666	C	-0.357	C	-0.119	C	0.000
		$H_{(2)}$	0.450	0.333	$H_{(2)}$	0.333	$H_{(3)}$	0.119	H	0.119	C	-0.357
					C	-0.357			C	-0.357	$H_{(3)}$	0.119
					$H_{(3)}$	0.119			$H_{(3)}$	0.119		

FIG. 1. Structure of the molecules used in the simulations and a description of their charge distributions. †As explained in the methods, we used the program SPARTAN™ to calculate an *ab initio*, atomic charge distribution for the quantum urea charge set. All other charge distributions were based on our own ENCAD potential parameterization. @Dipoles are given in units of debye and were calculated as an average over all molecules in the highest concentrated simulation at the time step closest to 900 ps. ¥For water, the dimer refers to two waters making one hydrogen bond. For urea, a dimer refers to the cyclic dimer potential energy for two urea molecules and was defined as consisting of two urea molecules each making a hydrogen bond from its carbonyl group to the *trans* hydrogen of the other urea. To calculate the minimum energy of the dimers, they were placed *in vacuo* and allowed to minimize over 2000 steps using ENCAD. All energies are given in kcal/mol. #Potential energies with water were calculated by forming a hydrogen bond between the water hydrogen and a solute molecule's oxygen group. In the case of isobutylene, which has no oxygen, water was placed near the exposed, sp^2 hybridized carbon. These complexes were then allowed to minimize as previously described. [a]All charges are given in units of electrons. For clarity in the charge distribution table, atoms are listed from the ''top'' of the molecule down, and the numbers in subscripts indicate the number of other atoms with that charge in the molecule. All simulations used the same values for the Lennard-Jones dispersion and repulsion parameters, which were empirically derived for simulations of protein in solution (Refs. 35, 36). The following table shows the minimum distance r_0 and minimum energy ϵ values for atoms used in the simulations

Atom, bonding	H	O, $sp2$	O, $sp3$	O, water	C, $sp2$	C, $sp3$	N
r_0 in Å	2.852 50	3.100 50	3.191 92	3.553 22	4.315 00	4.220 20	3.817 10
ϵ in kcal/mol	0.038 00	0.184 79	0.347 05	0.184 79	0.073 82	0.037 63	0.413 15

where m_{box} is the mass of the atoms in the box in atomic mass units (amu), V_w is the volume of water in a pure solution (29.89 Å^3, explained in Table I), and m_w is the mass of one water molecule (18 amu). For isobutylene, the volume was estimated using volumes from Harpaz *et al.*[49] The simulations used a 2 fs time step, a periodic box, and a smooth force-shifting truncation as used by ENCAD for protein[35] and pure water simulations.[41] The system was equilibrated to the running temperature of 298 K, and records were saved every 0.4 or 0.5 ps. Running on a DEC Alpha 3000 400 workstation, 1 ns of simulation required ~40 cpu h. We summarize the parameters used for each simulation including box size, density, and length of simulation in Table I.

Using the program SPARTAN™ (Wavefunctions Inc.), we calculated an *ab initio* set of atomic charges for urea using the CHELPG algorithm[50,51] and the 6-31 G** basis set.[52] The algorithm produces a charge distribution by fitting the electrostatic potential, and the calculations were run at the restricted Hartree–Fock level of approximation.

We used the Einstein relation[53] to measure the diffusion coefficient as a mass transport quantity. This calculates the squared distance traveled by a molecule from its initial position per unit time. For a molecule i at position $\mathbf{r}_i(t)$ from an initial position $\mathbf{r}_i(0)$, the diffusion coefficient D at time t is defined as

$$D_t = \frac{\langle |\mathbf{r}_i(t) - \mathbf{r}_i(0)|^2 \rangle_i}{6t},$$

where $\langle\ \rangle$ indicates an average over all i molecules. At each saved time step after the first 100 ps, we calculated a diffusion coefficient for every molecule using the position of a designated ''central atom.'' For example, we used the carbon for urea's diffusion and the oxygen for water's. For each molecule type, i.e., water or urea, we found an average diffusion coefficient and also a standard deviation about the mean. These values were then averaged over time steps past 100 ps to obtain an overall diffusion coefficient and standard deviation.

TABLE I. Simulation parameters.[a]

# solutes	# waters	Urea simulation parameters Molarity	Density[b]	Box side	Time
1	214	0.23	1.0021	18.65	1.0
2	212	0.48	1.0060	18.66	1.0
4	208	1.00	1.0139	18.69	1.0
4	204	1.02	1.0142	18.57	1.0
8	207	1.98	1.0288	18.93	1.0
8	198	2.06	1.0301	18.68	1.0
12	203	2.91	1.0430	19.10	1.0
16	200	3.76	1.0560	19.28	1.0
20	193	4.57	1.0684	19.37	1.0
25	192	5.46	1.0819	19.67	1.0
29	186	6.20	1.0933	19.77	1.0
32	183	6.71	1.1010	19.89	1.0
		Acetamide simulation parameters			
# solutes	# waters	Molarity	Density[c]	Box side	Time
1	213	0.23	0.9984	18.64	1.0
2	213	0.49	0.9993	18.73	0.2
4	206	1.01	1.0012	18.71	0.2
4	204	1.02	1.0013	18.65	0.2
8	209	1.92	1.005	19.13	0.2
8	199	2.00	1.0048	18.86	0.2
12	200	2.84	1.0079	19.22	0.2
16	196	3.66	1.0109	19.45	0.2
29	178	6.05	1.0196	20.01	0.2
32	181	6.38	1.0208	20.31	1.0
		Acetone simulation parameters			
# solutes	# waters	Molarity	Density[b]	Box side	Time
1	213	0.26	0.9960	18.65	1.0
2	212	0.51	0.9941	18.73	0.2
4	204	1.01	0.9901	18.71	0.2
4	203	1.02	0.9900	18.68	0.2
8	206	1.89	0.9832	19.17	0.2
8	193	2.00	0.9824	18.81	0.2
12	195	2.79	0.9762[d]	19.27	0.2
16	196	3.49	0.9707[d]	19.68	0.2
29	172	5.78	0.9526[d]	20.27	0.2
32	176	6.05	0.9505[d]	20.63	1.0
		Isopropanol simulation parameters			
# solutes	# waters	Molarity	Density[b]	Box side	Time
1	213	0.10	0.9949	18.66	0.2
2	209	0.47	0.9918	18.66	0.2
4	203	1.06	0.9868	18.71	0.2
4	203	1.06	0.9868	18.71	0.2
8	194	1.92	0.9792	18.89	0.2
8	207	1.99	0.9785	19.25	0.2
12	195	2.49	0.9738	19.32	0.2
16	197	3.12	0.9674	19.78	0.2
29	172	5.52	0.9392	20.45	0.2
32	172	5.90	0.9341	20.74	1.0
		Isobutylene simulation parameters			
# solutes	# waters	Molarity	Density[e]	Box side	Time
1	213	0.26	1.0003	18.62	0.3
32	175	5.84	0.9015	20.88	0.5

[a]Units used in the table; Molarity in mol/ℓ; density in g/ml; box side in Å^3; and simulation time in ns.
[b]Densities obtained from the 65th CRC (Ref. 48).
[c]Densities acquired from Christoffers *et al.* (Ref. 47).
[d]These densities were beyond experimental range, and were therefore extrapolated.
[e]Used following values for isobutylene and water volumes to calculate the density, isobutylene, 121.08 Å^3, and water, 29.89 Å^3. Isobutylene volume in water calculated from the volumes in Harpaz *et al.* (Ref. 49), while the water volume of 29.89 Å^3 was estimated by dividing the water's atomic mass by Avagrado's number and its density at room temperature.

We defined the existence of a hydrogen bond geometrically; the distance cutoff between a hydrogen and an acceptor atom was 2.6 Å and the angle between the acceptor, hydrogen, and donor atoms had to have been greater than 120°. Our definition of a hydrogen bond is quite stringent. Consequently, in a pure water simulation, we would find only 3.95 hydrogen bonds per water. Integration under the first peak of the experimental water oxygen-oxygen radial distribution function yields 4.4 bonds per water.[54] Hydrogen bond lifetimes were calculated by monitoring the existence of a hydrogen bond from each recorded time step. A lifetime is measured from the time that the bond was formed until it was broken.

We calculated the radial distribution function in the following manner. For a distribution function between atoms of type A and type B, distances were computed at each time step between all type A and B atoms. These distances were then sorted into a histogram with a specified bin width Δr (usually 0.10 Å) beginning at a distance of 0 Å and ending at 20 Å. An individual bin of the histogram $P(r_i)$ centered at a distance r_i was converted into a point in the function using the following relationship

$$g_{\mathrm{AB}}(r_i)=\frac{n(r_i)}{n(r_i)_{\mathrm{ideal}}},$$

where

$$n(r_i)=\frac{P(r_i)}{n_{\mathrm{ts}}\cdot n_A} \quad \text{and} \quad n(r_i)_{\mathrm{ideal}}=\rho_B\times V_{\mathrm{shell}}(r_i).$$

The number density $n(r_i)$ of B atoms around A atoms is the average number of distances in a bin per time step per atom of type A, or $P(r_i)$ divided by the number of time steps n_{ts} and number of A atoms n_{A}. The ideal number density $n(r_i)_{\mathrm{ideal}}$ of B atoms around A atoms is calculated from the density of type B atoms in the box ρ_{B} (number of B atoms divided by the box volume) multiplied by the shell volume $V_{\mathrm{shell}}(r_i)=4\pi r_1^2\times\Delta r$.

To show that our longer simulations provide better statistics, we calculated the 32 individual nitrogen–nitrogen radial distribution functions, $g_{\mathrm{NN}}(r)$, in the 3.76 M urea simulation (see Table I) for two time intervals; the first 100 ps after temperature equilibration to duplicate the length of earlier simulations and for the full 1 ns of the trajectory. For each interval, we averaged the 32 functions into an average $g_{\mathrm{NN}}(r)$ and also found a standard deviation of the mean that showed the spread of the functions.

To create a snapshot of the solution, we viewed all simulation trajectories on a Silicon Graphics Indigo 2 workstation using the program MOLMAN, which is able to read an ENCAD trajectory and display the time steps sequentially. The time step's coordinates were output and then imported into MACIMDAD™ (Molecular Applications Group) to generate PICT files for figures.

To calculate surface areas and intermolecular contacts, we used the Voronoi construction as implemented in Gerstein *et al.*[55] This construction surrounds each atom with an unique polyhedron, so that all points within the polyhedron are closer to the enclosed atom than any other. Faces of Voronoi polyhedra, consequently, are equidistant from two atoms, and they can be uniquely identified by the two atoms they separate. For each atom, we summed the total area of its faces and the facial area covered by a particular molecule type. These sums were used to find the fraction of a molecule's particular polyhedra area covered by a given type of molecule (solute and/or solvent). We averaged over all molecules and time steps after equilibration.

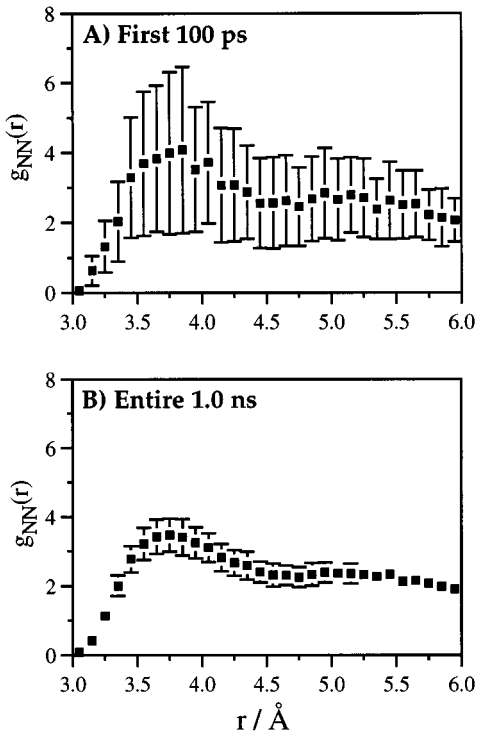

FIG. 2. Comparison of the $g_{\mathrm{NN}}(r)$'s calculated over different time intervals in the 3.71 M urea simulation. Both the mean and standard deviation (when averaged over the 32 nitrogens) are shown. (A) shows these values derived from the first 100 ps, while (B) shows them from the entire 1 ns simulation. Means are shown by solid squares and standard deviation by error bars. To display the deviations more clearly, we only show the region from 3.0 to 6.0 Å. If we presented the entire function from 0 to 20 Å, the width of the graph and the peak occurring at 2.15 Å due to the bonded, neighboring nitrogen would dwarf the fluctuations and obscure the point of this analysis.

III. RESULTS

A. Sampling statistics

Figure 2 illustrates how longer simulations give better statistical sampling than shorter ones. For each of the 32 nitrogens in the 16 urea (3.71 M) simulation, we calculated a nitrogen–nitrogen distribution $[g_{\mathrm{NN}}(r)]$ over two time intervals; the 100 ps after equilibration and the full 1 ns of the simulation. The figure shows a mean and a standard deviation derived from the 32 distributions at each point r. When a system is at equilibrium, we expect the deviation to decrease with longer simulation times as $\sqrt{t_s/t_l}$, where t_s and t_l are the lengths of the shorter and longer simulations, respectively. For our urea simulations, we find this expected behavior; the deviation from averaging over 1 ns is 28% of that

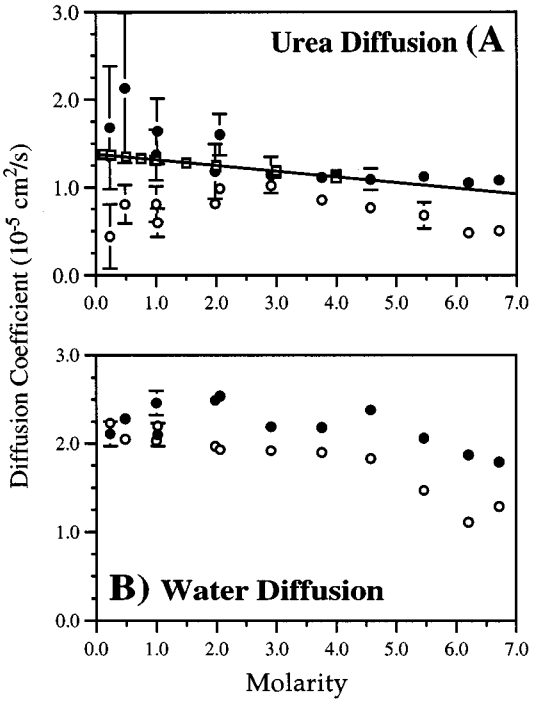

FIG. 3. Diffusion in urea solutions. Experimental values are shown with (□); values from the simulation using the simple charge set are represented by (●); and values from the simulation using the quantum charge set are represented by (○). (A) contrasts the urea diffusion coefficients from experiment to those found in our simulations. To compare simulation values outside of the experimental range, we extrapolated a straight line from the experimental diffusion coefficients. (B) shows the water diffusion coefficients from our simulations of urea solutions. For comparison, the experimental diffusion coefficient of a pure water solution is 2.3×10^{-5} cm^2/s (Ref. 61). In both parts, the error in the urea diffusion coefficient found from simulation tends to decrease as the urea concentration increases. This greater reliability of the diffusion coefficient is due to the increased number of ureas sampled during the calculation. For example, the simulation with 1 urea (0.23 M) has a standard deviation of almost a magnitude greater than the simulation with 32 ureas (6.71 M), 0.70×10^{-5} cm^2/s vs 0.09×10^{-5} cm^2/s, respectively. The data from the Gosting and Akeley experiment (Ref. 62) on the diffusion of urea in water were incorrectly reported in Landolt and Börnstein (Ref. 56). A constant relating the diffusion coefficient to its concentration was given instead. The data found by Albright and Mills (Ref. 63) and the correct experimental diffusion coefficients from Gosting and Akeley are plotted in (a) and listed below in units of 10^{-5} cm^2/s.

Molarity	0.10	0.13	0.25	0.50	0.75	0.98	1.00	1.50	2.00	3.00	4.00
Gosting and Akeley		1.373	1.363	1.343	1.326	1.309	1.307	1.274	1.245	1.189	1.143
Albright and Mills	1.374		1.370	1.344			1.305		1.234	1.165	1.107

from averaging over 100 ps, and this decrease is nearly the same as the 32% expected. Thus, analysis of deviations indicates that our system has reached equilibrium by 100 ps.

Note, however, that being at equilibrium does not preclude the need to collect sufficient statistics for accurate results, and the drop in deviation illustrates this point. Consequently, Åstrand *et al.*'s simulations[32] may have been at equilibrium, but they were not long enough to provide comparable statistical sampling to our simulations.

B. Diffusion

In Fig. 3, we compare the experimental urea diffusion coefficients to ones we determined from our simulations. Our values for both charge sets faithfully reproduce the trend in the experimental values; increasing the urea concentration slows its diffusion. This progression makes sense since pure urea exists as a solid at room temperature suggesting that the diffusion in concentrated solutions is very slow. A line fit through the experimental diffusion coefficients usually falls within one standard deviation of the values calculated from simulations which use the simple charge set. However, all the urea diffusion coefficients from simulations using the quantum charge set do not come within a standard deviation of the line derived from the experimental values. Moreover, diffusion with the quantum charge set is always slower than with the simple charge set. The lower portion of the figure compares the water diffusion coefficients found from the two series of urea runs. Increasing urea concentration retards water diffusion; however, this effect is much more prominent in simulations using the quantum charge set.

For the other solutes, we compare simulation versus experimental diffusion coefficients in Fig. 4. Although most of the solute runs simulated a shorter period of time than the urea ones (see Table I), they are within acceptable agreement of the experimental numbers. More importantly, the runs simulated for longer times and with more solute molecules exhibit solute diffusion coefficients that are generally closer to experiment than the shorter runs with less solute molecules. For water diffusion, we have only been able to find experimental values from studies of acetone solutions.[56] Comparison with this data shows that water diffusion coefficients from our simulations successfully approximate experimental values. We find these results quite encouraging. Because we use a general parameterization based on previous protein simulations, we assume that similar groups on different solutes have the same attributes. Although Meier and Coussens[43] have shown this to be an oversimplification, our method is still able to reproduce the experimental diffusion of the solutes quite accurately.

We would like to explain an apparent contradiction in our results. The more polar, quantum charge set slows the diffusion of both urea and water (Fig. 3). In contrast, as shown in Fig. 4, simulations with the other solutes indicate that increasing a solute's polarity increases its diffusion. As described in Fig. 1, these solutes used charge distributions that are not nearly as strong as the one used by the quantum charge set ureas. Comparing the diffusion from these two types of charge distributions is misleading, because they interact in solution much differently as discussed in the next section.

C. Hydrogen bonding

In Fig. 5, the two representations of part A show that the total number of water hydrogen bonds decreases for increasing concentrations of solutes other than urea and that this effect becomes more pronounced the more hydrophobic the solute is. We expect such behavior, since we are introducing more nonpolar groups with which water cannot hydrogen bond. On the other hand, increasing the molarity of urea

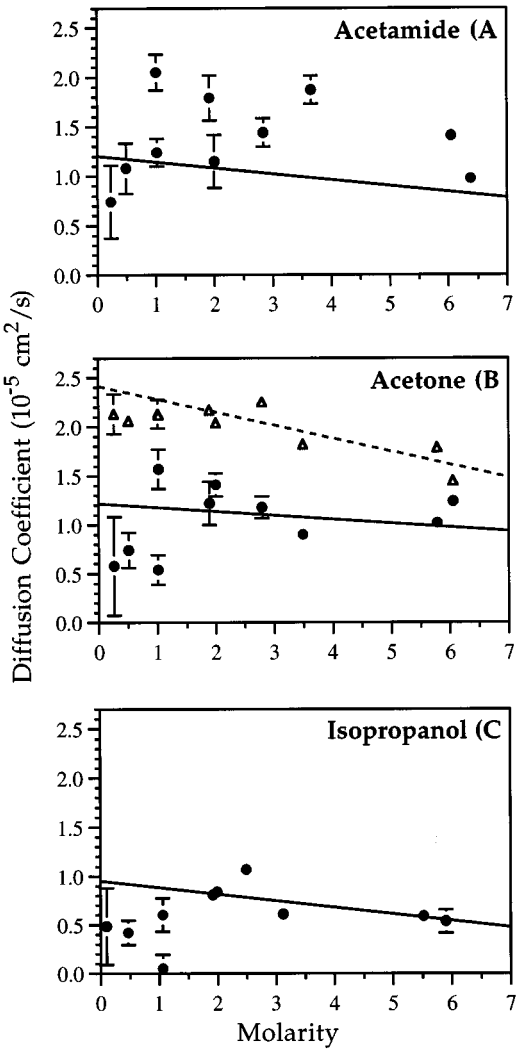

FIG. 4. Diffusion in solute solutions. All experimental values of the above diffusion coefficients were obtained from Landolt–Börnstein (Ref. 56). (A) compares the acetamide diffusion coefficients found from simulation, denoted by the (●), with experiment, shown by the solid line. (B) compares the experimental and simulation diffusion coefficients for both water and acetone. Simulation values for water are given by the (△) and for acetone by (●). Experimental values are again shown by lines; the broken line represents experimental water values and the solid line represents experimental acetone ones. (C) shows the diffusion coefficient for isopropanol from experiment, the solid line, and from our simulations, the (●). As in Fig. 2, the standard deviation exhibits the same decrease with increasing concentration as seen with the urea simulations.

solutions causes water to make more hydrogen bonds, with the quantum charge set inducing more water hydrogen bonding than the simple charge set. To investigate the difference in water hydrogen bonding between urea and the less polar solutes in more detail, we categorized the types of hydrogen bonds made by water. In Fig. 5(b), the simulations generally show a decrease in the number of water–water hydrogen bonds with increasing concentrations of solute. Furthermore, contrary to the trend shown for total water hydrogen bonds, the more hydrophilic a solute is, the more it lowers the amount of water–water hydrogen bonding. The urea simulations demonstrate this phenomenon most clearly with the greatest decrease caused by the quantum charge set. As shown in Fig. 5(c), the urea makes up for its lack of water–water hydrogen bonds with water–solute hydrogen bonds. Therefore, although the less polar solutes allow water to make more water–water hydrogen bonds, they cannot make as many water–solute hydrogen bonds, which creates an overall decrease in the total number of water hydrogen bonds. In contrast, urea increases the total number of water hydrogen bonds because of its ability to form more water–solute hydrogen bonds.

Figure 5(d) displays the average number of hydrogen bonds made by each solute molecule. Increasing the concentration of acetamide, acetone, and isopropanol decreases the number of solute hydrogen bonds. One explanation of this effect is that these solutes aggregate and thus sequester their hydrogen bonding groups from water. For urea, increasing the concentration has little effect.

Ureas using the quantum charge set make more hydrogen bonds than the ureas using the simple set. This is understandable as one might expect that increasing the polarity of a molecule would increase its hydrogen bonding. Not so easily rationalized is the contrary behavior of the two charge sets shown in Fig. 5(d); increasing the concentration of ureas with the stronger dipole slightly decreases the total number of urea hydrogen bonds, whereas ureas using our simple charge set increase their number of hydrogen bonds with increasing concentration. To explain these differences, Figs. 5(e) and 5(f) show the breakdown of urea's hydrogen bonds for each charge set. In Fig. 5(e), we can see that ureas using the quantum charge set form more urea–water hydrogen bonds, but as shown in Fig. 5(e), the urea the using simple charge set make more urea–urea hydrogen bonds. This last result is particularly interesting since it is directly related to the formation of urea dimers. In simulations at the highest concentration, the simple charge set forms over twice the number of urea–urea, ''dimer,'' hydrogen bonds as quantum charge set.

We calculated average hydrogen-bond lifetimes for all simulations and categorized them according to donor–acceptor pairs. In general, hydrogen-bond lifetimes were very similar between solutes. The simulation of pure water possessed an average lifetime of about 2 ps. In the solute simulations, water–water hydrogen-bond lifetimes lasted from between 10% to 20% longer and showed a small increase with increasing concentration of solute. For all other cases (e.g., water–solute), the hydrogen-bond lifetimes were very similar for solutes other than urea. Isopropanol was the only exception with lifetimes sometimes 10 times longer than the other solutes (data not shown).

Table II contrasts hydrogen-bond lifetimes between the two urea charge sets. As mentioned in the previous paragraph, lifetimes of hydrogen bonds made from a water oxygen to a urea hydrogen are almost the same for the two charge sets. The major disparity is in lifetimes involving urea's oxygen and a water's hydrogen. In urea simulations using the simple charge set, this type of hydrogen bond lasts on average about 1.5 ps. As the concentration of urea increases, the quantum charge set simulations steadily increase

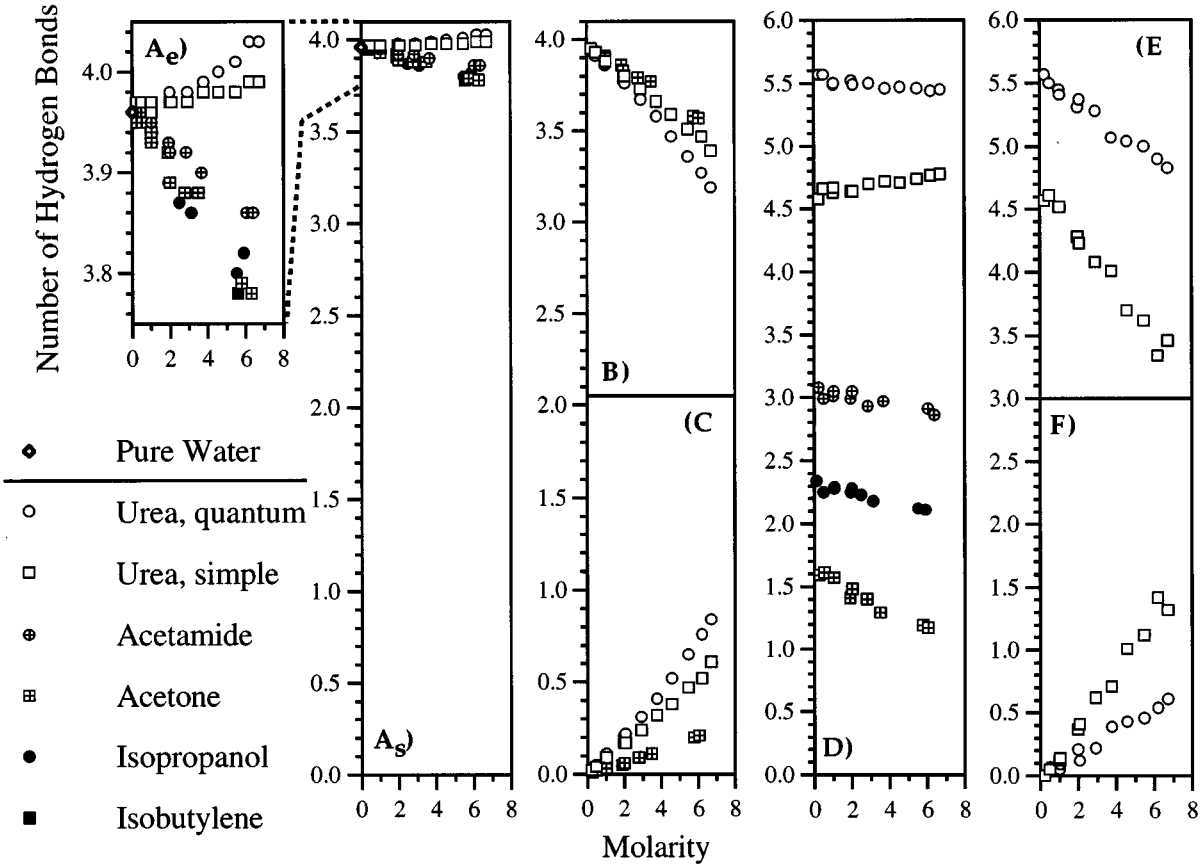

FIG. 5. Hydrogen bonding in each of the highest concentration solution solutions. (A) depicts the total number of water hydrogen bonds and is shown twice using different scaling. (a_s) shows the graph on the same scale as (B) and (C) for comparison, while (a_e) enlarges the region from 3.75 to 4.05 to aid in distinguishing trends. As explained in the Methods, our hydrogen bond definition is so stringent that we do not find the experimental 4.4 bonds per water in the pure water simulation. (B) is the average number of hydrogen bonds formed between waters. (C) displays the number of hydrogen bonds between a water and a solute molecule made per water. In (B) and (C), we only compare the results from three series of simulations for clarity; the urea simulations using the simple charge set, the urea simulations using the quantum charge set, and the acetone simulations. Please note that (A) is the sum of (B) and (C). (D) shows the total number of hydrogen bonds made per solute molecule. Since isobutylene cannot form any hydrogen bonds, those runs were left out of the figure. For acetamide, acetone, and isopropanol, the average number of hydrogen bonds that they make directly reflects their ability to hydrogen bond. Acetamide can form the most hydrogen bonds with its carbonyl and amide groups (see Fig. 1). Isopropanol's hydroxyl group forms more hydrogen bonds than acetone's lone carbonyl group. So, in the simulations, the solutes rank in the above order from the most hydrogen bonds made by acetamide to none made by isobutylene. (E) displays the average number of waters hydrogen bonded to a solute. (F) is the average number of solutes making hydrogen bonds with another solute. In (E) and (F), we only show numbers for the two charge sets of urea since the other solutes did not show any significant trends. As with (A), (D) is the sum of (E) and (F). All values calculated per time step.

the hydrogen-bond lifetimes between the urea oxygen and the water hydrogen to almost 4 times the value of the simple charge set. For urea dimers and oligomers, the quantum charge set gives lifetimes that are on average ~30% longer than those from the simple charge set.

D. Radial distribution functions

1. Comparison of simulation with experiment

In Fig. 6, we compare radial distribution functions found from neutron diffraction experiments[21,22,57] with ones calculated from our simulations. Figure 6(a) shows the total nitrogen centered (N-centered) radial distribution functions. This quantity measures the total number of all types of atoms (carbon [C], hydrogen [H], nitrogen [N], and oxygen [O]) within a certain distance of a nitrogen. As seen in the figure, the N-centered distribution is essentially the same for simulations using the simple charge set and for those using quantum charge set. This is also true for the other radial distribution functions. Therefore, we will only discuss the distributions from the simple charge set simulations, and further comparisons with experiment will only show distributions from those simulations.

Overall, the experimental and simulation N-centered curves are similar in appearance. The main difference is in the height and location of the first peak, which is higher and closer for the curves from simulation. This probably reflects a closer N···H spacing in the simulation. Such discrepancies have been reported in other simulation studies.[29,32] We also show distribution functions for the H–H and H–(O,C,N) spacings in Figs. 6(b) and 6(c), respectively. These distribution functions more closely match experiment than the N-centered distribution discussed above. Still, the simulation results tend to have sharper peaks than the experimental curves.

TABLE II. Hydrogen bond lifetimes for urea simulations.[a]

Molarity	0.23	0.48	1.00	1.02	1.98	2.06	2.91	3.76	4.57	5.46	6.20	6.71
						Urea oxygen–urea hydrogen						
simple	···	1.10	0.90	0.94	0.91	0.89	0.97	0.94	0.98	0.99	1.03	1.02
quantum	···	2.04	1.14	1.22	1.44	1.23	1.27	1.30	1.35	1.27	1.37	1.37
						Urea oxygen–water hydrogen						
simple	1.39	1.57	1.55	1.58	1.57	1.62	1.62	1.70	1.68	1.74	1.80	1.78
quantum	4.97	5.08	4.75	5.28	5.60	5.18	5.49	5.45	5.71	5.79	6.76	6.33
						Water oxygen–urea hydrogen						
simple	0.62	0.76	0.75	0.77	0.75	0.75	0.78	0.79	0.79	0.80	0.82	0.81
quantum	0.99	0.97	0.98	0.96	1.01	0.98	1.03	1.02	1.06	1.07	1.13	1.12

[a]Molarity is given in units of mol/ℓ and all lifetimes are reported in picoseconds.

2. Water structure

Figure 7 displays the water oxygen–oxygen (O–O) radial distribution function from various simulations. This function measures how well a solute mixes with water. As explained in the methods, the radial distribution function at a particular distance is the actual number density divided by the number density of a perfectly distributed system. In this case, if the waters are well mixed with the solute, then the closer the distribution would be to pure water. Figure 7(a) shows the water O–O distribution functions from simulations using the quantum charge set, while Fig. 7(b) shows functions from simulations using the simple charge set. As with the other distributions, they are quite similar to each other. Also, even at the highest concentration, urea does not seem to affect the water O–O distribution much in comparison to pure water, which indicates that urea disperses well in solution. As the solute molecules become less polar, the more they disturb the water O–O distribution [see Fig. 7(c)]. Features up to 10 Å are shifted up, while past 10 Å, the curve dips below 1 to compensate for the local enhancement. In effect, these attributes indicate that the water and solute are separating from each other as the hydrophobicity of the solute increases, suggesting that the less polar solutes aggregate in proportion to their degree of hydrophobicity, in contrast to urea which remains well mixed with water.

E. Aggregation/solvation

As the hydrophobicity of the solute increases, the aggregation of solute creates an actual phase separation. We see this phenomena clearly for the most concentrated isobutylene solution in comparison to the urea solution at a similar concentration (Fig. 8). To measure the degree of aggregation, we calculated the fraction of a molecule's surface area covered by other solute and solvent molecules. To calculate surface areas, we used the Voronoi polyhedra construction as described in Gerstein *et al.*[55] Because this construction associates with each nearest neighbor a unique patch of ''contact area,'' it allows a more precise definition of the extent of coverage than simply counting neighbors within a distance cutoff.

Table III sums up our results for the simulations containing 32 solute molecules. The better a solute mixes with water, the greater a fraction of a water molecule's surface it covers on average. As expected, the most polar solute (urea using the quantum charge set) covers the greatest fraction of a water's surface, and decreasing the solute's polarity lowers this fractional coverage. Conversely, the more a solute tends to aggregate, the more it contacts and covers other solute molecules instead of water. This trend is evident as the solutes become less polar. To provide a point of reference, we calculated a hypothetical, percentage solute–solute surface area for a pure water simulation (for more detail, see the legend to Table III). Values larger than this hypothetical, water surface area is a good indication of how well a solute is aggregating. We find it surprising that the quantum charge set urea has a value less than the hypothetical water one. This indicates that the quantum charge set urea is somehow resisting aggregation by surrounding itself with water molecules. Being the least polar, isobutylene shows the greatest amount of self-interaction. In fact, over its entire trajectory, the isobutylene simulation possessed a substantial population of solute molecules completely sequestered from water (about 20 times the value from any other solute simulation). Converting this value into something more tractable, we find that at almost every time step there was one isobutylene completely surrounded by other isobutylenes.

This result suggests that not only did isobutylene aggregate, but it actually created a separate hydrophobic ''phase'' from water. If so, then we expect to find two species of isobutylene molecules; one at the water–solute interface and a second partitioned from water in the hydrophobic, solute phase. A histogram of the average fraction of a solute's surface area covered by other solute molecules (Fig. 9) clearly shows these two populations in the isobutylene simulation. Isobutylenes with ~79% of their surface contacting other isobutylenes interacted with water at the interface, whereas isobutylenes in the second population caused the noticeable spike at 100%. The other solutes were like urea in that they did not contain significant numbers of molecules completely separated from water (Table III).

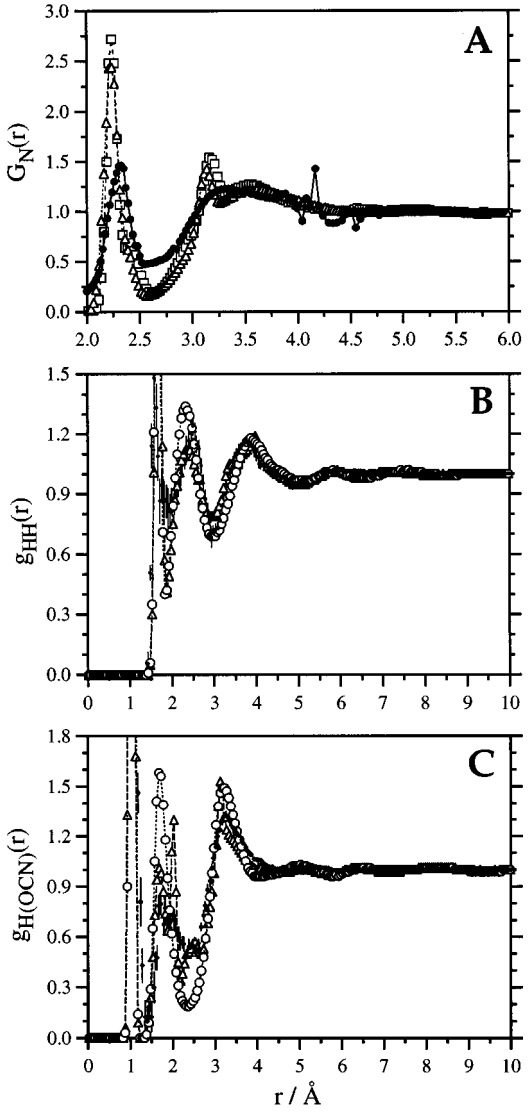

FIG. 6. Comparison of experimental vs simulation radial distribution functions. All experimental data was taken from Turner *et al.* (Ref. 22). (A) Nitrogen centered radial distribution functions, $G_N(r)$, compared between our 6.71 M urea simulations using the simple charge set, (△), and the quantum charge set, (□), with a 7 M neutron diffraction experiment, (●). The neutron diffraction experiments were performed with N_{15} substituted urea and D_2O, which might explain some of the differences between the simulation and experimental curves. The features past 4.0 Å have been attributed to truncation ripples (Refs. 29, 64) (B) shows the H–H radial distribution function, $g_{HH}(r)$, and (C) shows the H–(O,C,N) radial distribution function, $g_{H(OCN)}(r)$. For both, the neutron diffraction study used a 10 M solution and curves are shown by (•) with error bars. Although we did not perform a simulation very close to the experimental 10 M solution, we show distributions for 0.23 M, (○) and 6.71 M, (△), urea simulations so that a trend can be seen.

IV. DISCUSSION

A. Choice of urea potential

As explained previously, Åstrand *et al.*[32] have argued that a more realistic, urea dimer energy of about −20 kcal/mol would favor formation of complexes in solution. In order to test this idea, we have run equivalent series of simulations using a simple charge set or a quantum charge set for the urea molecule (Fig. 1). The quantum charge set, which has a dimerization energy about twice that of the simple charge set, more closely models the actual urea dimer energy. Nevertheless, radial distribution functions show that both sets produce nearly equivalent solution structures which are very similar to experimental curves (Figs. 6 and 7). This is in agreement with the work of Chipot *et al.*,[58] who studied the effects of various charge distributions in simulations of polar molecules in water and found that more complex or stronger charge distributions did not offer any significant advantage over a simple charge distribution.

Dynamically, using the simple charge set approximates experimental diffusion coefficients better than using the quantum charge set (Fig. 3). Moreover, other simulations, which used polarizable potentials and *ab initio* charge sets, were also unable to reproduce the experimental diffusion coefficients. For example, using a urea charge set with a dimer energy of around −20 kcal/mol, Tanaka *et al.*[25] and Åstrand *et al.*[32] both found diffusion of urea to be less than the experimental values. Additionally, they noted a decrease in water mobility near urea molecules. Our analysis of hydrogen bond numbers and lifetimes support these findings. We find that the quantum charge set ureas spend more time complexed to a larger number of waters than ureas using the simple charge set (Table II and Fig. 5). As a result, the number of hydrogen bonds between ureas reveals that using the weaker, simple charge set for urea, surprisingly, favors dimer formation.

We can explain these results if we consider the strength of the various interaction energies. For clarity, we summarize the interaction energies from the two types of urea solutions in Table IV. In our system, using the quantum charge set not only doubles the strength of urea–urea interactions, but it also increases the strength of urea–water interactions. The water–water interaction remains the same. Therefore, as long as there is an excess of water (at 6.71 M, the ratio is about 6 waters for every urea), the solution is better off forming urea–water complexes at the expense of water–water ones. As a result, a urea molecule will make more contacts with water, which consequently inhibits urea dimerization. Figure 5, which shows the breakdown of the hydrogen bonding patterns, clearly illustrates this. The imbalance of intermolecular energies also increases the amount of time a urea spends complexed to water as indicated by longer hydrogen bond lifetimes (Table II).

In other simulations using quantum charge sets and potentials, we believe that the same situation occurs. The basis for our reasoning is shown in Table IV, which additionally lists the intermolecular energies from Åstrand *et al.*'s urea simulations[32,42] and shows that the ratios between their intermolecular energies are similar to our quantum set. The urea–urea interaction is ~4 times stronger than the water–water interaction, and the urea–water interaction is twice the strength of the water–water interaction. As in our quantum charge set simulations, these unbalanced energies most likely explain why Åstrand *et al.* did not find more urea complexation and their diffusion was so low.

With the ENCAD potential, using the simple charge set

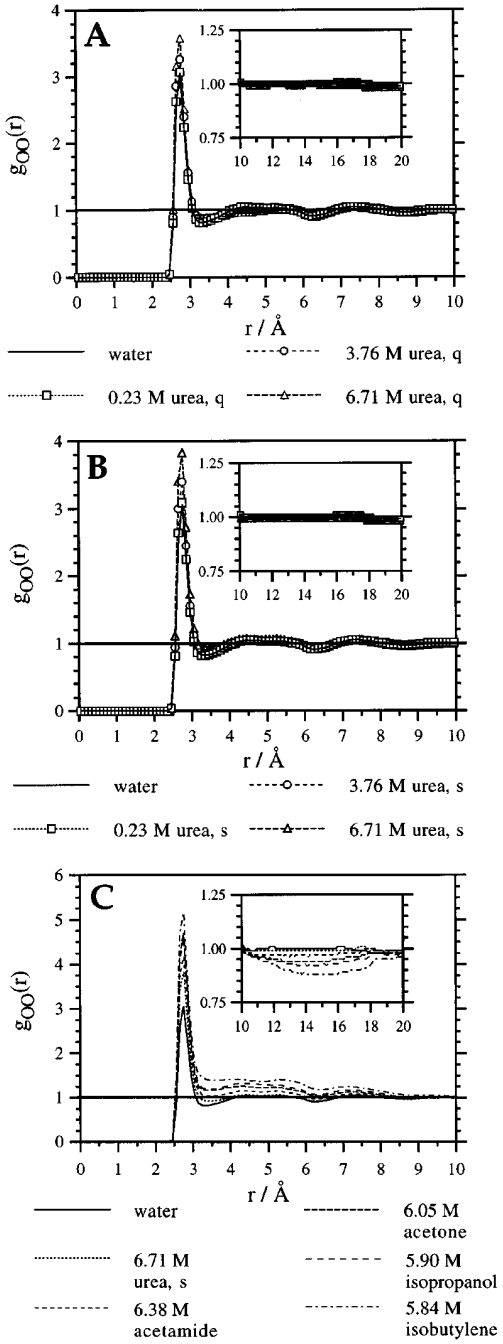

FIG. 7. Comparison of the experimental and simulation water oxygen–oxygen radial distribution function $g_{OO}(r)$. In all the parts, the inset shows the $g_{OO}(r)$ from 10 to 20 Å. The legend for each graph is shown below it. In each legend, an *s* denotes the simple charge set, while a *q* represents the quantum charge set. (A) compares a $g_{OO}(r)$ from a pure water simulation to those found in the urea simulations using the quantum charge set. (B) is the same comparison with the urea simulations using the simple charge set. Except for the quantum charge set urea, (C) contrasts all the water $g_{OO}(r)$'s from the highest concentration solute simulations with the pure water distribution. To point out the correlation between the stepwise perturbation of the water $g_{OO}(r)$ and the degree of hydrophobicity of the solute, we show the values of the first peak, the first trough [as defined from the experimental, pure water $g_{OO}(r)$], and the approximate middle of the dip past 10 Å in the following table. All headings correspond to the concentration and type of simulation specified in the legend to (C).

Feature	r/Å	Water	Urea, simple	Acetamide	Acetone	Iso-propanol	Iso-butylene
First peak	2.75	3.05	3.83	4.17	4.70	4.63	5.16
First trough	3.35	0.82	0.92	1.04	1.17	1.20	1.42
''dip''	14.95	1.00	0.99	0.97	0.94	0.92	0.88

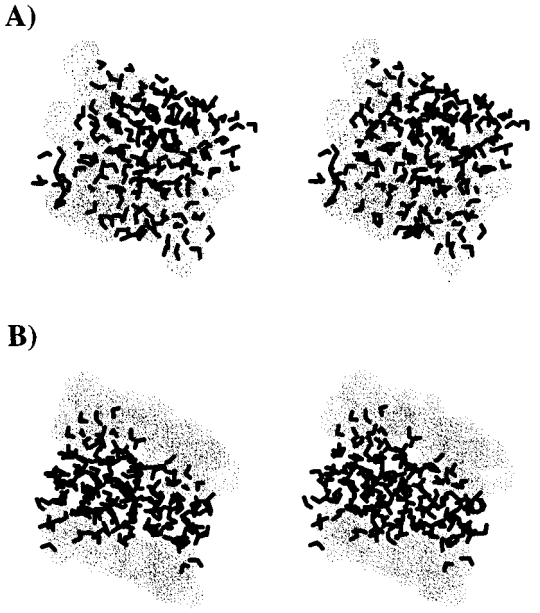

FIG. 8. Snapshot of the periodic box at 450 ps. The sticks represent water molecules and the dot surfaces indicate where the solute molecules are located. (A) shows the 6.71 M urea simulation, while (B) shows the 5.84 M isobutylene simulation.

for urea produces similar intermolecular energies for all three types of associations in solution. Therefore, one interaction is not favored over the other. Experiments measuring the strength of hydrogen bonds in urea solutions support such a model.[13,59,60] The nearly equivalent intermolecular energies allows the simple charge set to reproduce the solution's energetic and dynamic qualities more accurately. As mentioned earlier, radial distribution functions from the simple charge set are as close to experimental curves as those from the quantum charge set. For these reasons, we believe that in our system, the simple charge set derived from the ENCAD potential parameterization is better suited for further studies with proteins.

B. Assessment of urea models

Our results do not directly support either of the thermodynamic models. The SKSS model is based on urea forming dimers and oligomers in solution, but we do not find any substantial aggregation of urea. As mentioned earlier, using a more polar, *ab initio* charge distribution for urea in an attempt to induce dimer formation actually inhibits urea–urea dimers and instead promotes urea–water interactions (Fig. 5). In fact, we do find solute–solute complexes in our simulations, but they occur more often for the less polar solutes. As these solutes increase their degree of hydrophobicity, the more they aggregate in solution (Table III and Figs. 7, 8, and 9), and of all the solutes, urea aggregates the least because of its ability to hydrogen bond. Since the SKSS model attributes all of the increase in enthalpy of a solution to urea–urea hydrogen bonds, it does not consider other interactions. Such an oversimplification suggests how our results can support this model. The SKSS model implies that urea adds

TABLE III. % covered surface area of solutes.[a]

	Water[b]	Urea, quant 6.71 M	Urea, simple 6.71 M	Acetamide 6.38 M	Acetone 6.05 M	Isopropanol 5.90 M	Isobutylene 5.84 M
Average percentage of a solute molecule's surface covered by another solute (s.d.)	31 (16)	27 (11)	38 (15)	47 (18)	57 (18)	59 (16)	69 (16)
Percent of solute molecules completely surrounded by other solutes	0	0	0	0.0034	0.17	0.031	3.4
Average percentage of a water molecule's surface covered by solute (s.d.)	31 (16)	26 (15)	23 (15)	22 (17)	21 (16)	21 (19)	17 (15)

[a]Table III shows data from the most concentrated solutions of each solute. For reference, the molarity of each solution is reported underneath each heading. Standard deviations are noted as s.d. in the row headings and are shown in parentheses for each value.
[b]For reference, we calculated percent surface areas in a pure water simulation. We marked a number of waters occupying the same volume percent as the urea in the 6.71 M simulation (~30% by volume). These marked waters were treated as if they were solute molecules, and we performed the same analysis on this system as with the other molecules. The water simulation is completely distributed, which explains why we get the same values for the fraction of surface area covered by marked water around a marked water molecule vs an unmarked water molecule. In the calculations on the water simulation, we did not connect waters together, but treated them independently.

hydrogen bonds to the solution, but assigns them all to urea–urea interactions. As seen from the hydrogen bond data in Fig. 5, urea increases the total number of hydrogen bonds in the solution. If we only consider this quantity, then in this indirect manner, our data supports the SKSS model. Even though this explanation of aqueous urea is quite simplistic, it is sufficient to describe the thermodynamic data and is useful as point of departure from which to develop future concepts involving urea's interactions in solution.

As for the FF model, we find that urea affects water structure, but not exactly in the same manner as the model proposes. In the FF model, water exists in two states (ordered or disordered) and that by interacting with only the disordered water, urea increases the disordered population. If we apply the logic of the FF model to the other solutions with less polar solutes, we would expect them to have more ordered waters than a urea solution at a similar concentration. In a binary solution, the two states of water can be thought of as those interacting with solute (disordered) and those that do not (ordered). Our classification does not identify the disordered waters as in a denser or more compact state like the FF model suggests. Because the less polar solutes aggregate more than urea (Table III and Figs. 7, 8, and 9), these simulations partition the solution into water rich and solute rich phases. The separation allows fewer waters to interact with the solute and more waters to be tetrahedrally coordinated with each other. In contrast, we find that urea preserves the water distribution by dispersing evenly with water in solution. This finding agrees with previous simulations that found that the addition of urea does not significantly perturb the water distribution.[25,29,30,32] The water hydrogen-bonding pattern in Fig. 5 and the surface area coverage data in Table III show that the less polar a solute is, the more the water in solution interacts with itself. Therefore, urea, being the most polar, allows the least amount of water self-association, because, of all the solutes, it interacts the most with water. In terms of the FF model, there are more waters in contact with urea (disordered waters) and less in bulk (ordered waters) than in the other solute solutions. Thus, our results can also support the FF model.

Both models can be correct, and to a certain degree, each must possess some element of the truth since they are both able to explain the thermodynamic data. Furthermore, the mixed experimental results also suggest that each model has some validity. To reconcile two seemingly opposing views, we propose that both models approach the same phenomenon from mutually exclusive perspectives. The SKSS model explains urea's aqueous properties in terms of its abil-

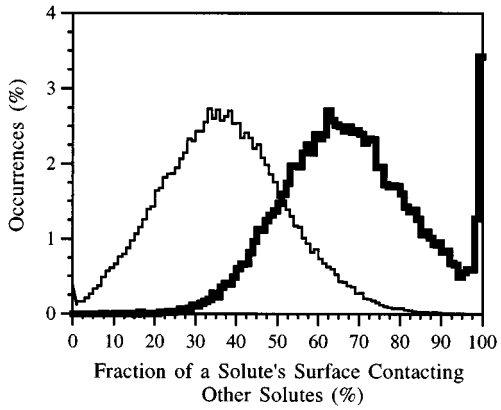

FIG. 9. Percent coverage of a solute's surface by other solutes. The thin line represents the distribution of the percent surface area covered by other solute molecules for the 6.71 M urea simulation using the simple charge set. The thick line shows the same for the 5.84 M isobutylene run. Both histograms were normalized by their respective total number of counts.

TABLE IV. Interaction energies in urea solutions.[a]

Interaction	Simple	Quantum	Åstrand *et al.*[b]
Urea–urea	−8.3	−16.3	−21.9
Urea–water	−7.7	−12.0	−11.2
Water–water	−7.2	−7.2	−4.7

[a]All energies given in kcal/mol.
[b]References 32 and 45.

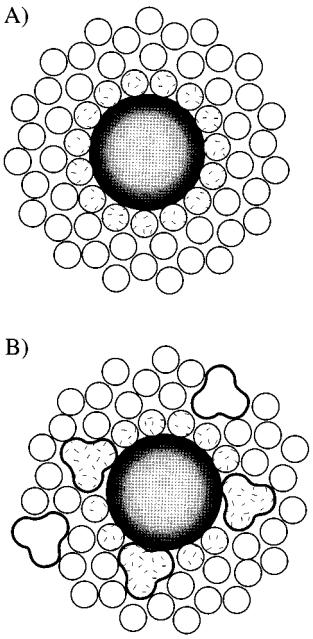

FIG. 10. Two dimensional representation of solutions around a hydrophobic sphere. (A) schematically represents in two dimensions a hydrophobic sphere in a solution of water. The hydrophobic sphere is a large and shaded circle in the middle, while the other smaller circles are waters. The stippling of the small circles marks the 15 water molecules in contact with the hydrophobic sphere. (B) shows the same hydrophobic sphere, but this time in a solution of aqueous urea. Ureas are represented by the boldly bordered, trefoil shapes. As in (A), the stippling marks the molecules in contact with the hydrophobic sphere. Urea mixes well with water and can displace water molecules from the hydrophobic surface. As a result, the sphere affects fewer molecules; 12 molecules (9 waters plus 3 ureas) in (B) vs 15 molecules in (A). Thus, the hydrophobic sphere orders less of the urea–water solution than it does pure water.

ity to hydrogen bond, whereas the FF model associates those properties with changes in liquid structure, which result from urea's ability to hydrogen bond.

C. Why urea is a denaturant

With respect to solvent denaturation, Nozaki and Tanford[8] have proposed an explanation for our data. Because urea is able to mix with water without severely disrupting its native structure, they believe that urea is able to incorporate into water's liquid lattice and form mixed clathrate structures. Jencks and co-workers[7,9] expanded on this idea by suggesting that urea lowers the free energy of cavity formation for hydrocarbons in water. If the hydrocarbons are small enough to fit into cavities made by water alone, then adding urea to the solution would not increase their solubility. Wetlaufer *et al.*[5] showed this effect for methane and ethane, and Nozaki and Tanford[8] reported the same for the amino acid glycine. Finding that urea replaces three waters at a solvation interface, Kuharski and Rossky[27] suggested that this release of waters helps urea lower the free energy of cavity formation. They also found ''that urea is not incorporated into the clathratelike structure around an apolar solute without significant distortion of this structure.'' We agree with their first point, but our results suggest that urea in solution minimizes the amount of disruption caused by apolar solutes. In sum, the ability of urea to hydrogen bond is important in preserving the structural integrity of water when apolar solutes are introduced. Urea also minimizes the entropy lost in creating the solvation shell by replacing three of the first shell waters with a fixed, planar structure that pays less of an entropic price in forming a hydrophobic interface (Fig. 10).

V. CONCLUSION

In our simulations of urea solutions, we have shown that a simple charge distribution for urea used with our ENCAD potential reproduces the structural and dynamic characteristics of a urea solution better than a quantum calculated charge distribution. Comparing the urea simulations to similar simulations of Y-shaped analogs, we show that urea tends to distribute evenly in solution, whereas the other molecules are more disposed to aggregate depending on their degree of hydrophobicity; the less polar a molecule is, the more it aggregates. Applying Voronoi polyhedra in our analysis of near neighbors, we found that the most hydrophobic analogue (isobutylene) formed a phase separation with water. These results show that the common models for urea solutions are both correct, since they describe different aspects of the same phenomenon. Furthermore, because urea mixes so well with water, we believe that urea denatures proteins by decreasing the free energy required to solvate a hydrophobic residue. To investigate urea's involvement at the solvation interface, we plan further urea simulations involving peptides and eventually proteins.

ACKNOWLEDGMENTS

J.T. and M.L. acknowledge the support from the NIH (Grant No. GM 41455), while M.G. acknowledges the support from a Damon-Runyon Walter-Winchel Fellowship (DRG 1272).

[1] R. H. Stokes, Aust. J. Chem. **20**, 2087 (1967).
[2] J. F. Brandts and L. J. Hunt, J. Am. Chem. Soc. **89**, 4826 (1967).
[3] G. I. Makhatadze and P. L. Privalov, J. Mol. Biol. **226**, 491 (1992).
[4] W. Brunig and A. Holtzer, J. Am. Chem. Soc. **83**, 4865 (1961).
[5] D. B. Wetlaufer, S. K. Malik, L. Stoller, and R. L. Coffin, J. Am. Chem. Soc. **86**, 508 (1964).
[6] S. J. Gill, J. Hutson, J. R. Clopton, and M. Downing, J. Phys. Chem. **65**, 1432 (1961).
[7] D. Robinson and W. P. Jencks, J. Am. Chem. Soc. **87**, 2462 (1965).
[8] Y. Nozaki and C. Tanford, J. Biol. Chem. **238**, 4074 (1963).
[9] M. Roseman and W. P. Jencks, J. Am. Chem. Soc. **97**, 631 (1975).
[10] J. A. Schellman, Comp. Rend. Trav. Lab. Carlsberg, Ser. Chim. **29**, 223 (1955).
[11] G. C. Kreschek and H. A. Scheraga, J. Phys. Chem. **69**, 1704 (1965).
[12] H. S. Frank and F. Franks, J. Chem. Phys. **48**, 4746 (1968).
[13] E. G. Finer, F. Franks, and M. J. Tait, J. Am. Chem. Soc. **94**, 4424 (1972).
[14] X. Hoccart and G. Turrell, J. Chem. Phys. **99**, 8498 (1993).
[15] R. Adams, H. H. M. Balyuzi, and R. E. Burge, J. Appl. Crystallogr. **10**, 256 (1977).
[16] F. Grieser, M. Lay, and P. J. Thistlethwaite, J. Phys. Chem. **89**, 2065 (1985).
[17] Y. Mizutani, K. Kamogawa, K. Nakanishi, J. Phys. Chem. **93**, 5650 (1989).

[18] M. Bloemendal and G. Somsen, J. Am. Chem. Soc. **107**, 3426 (1985).
[19] H. Piekarski and G. Somsen, Can. J. Chem. **64**, 1721 (1986).
[20] U. Kaatze, H. Gerke, and R. Pattel, J. Phys. Chem. **90**, 5464 (1986).
[21] J. L. Finney, A. K. Soper, and J. Turner, Physica B **156-157**, 151 (1989).
[22] J. Turner, J. L. Finney, and A. K. Soper, Z. Naturforsch. Teil A **46a**, 73 (1991).
[23] G. Jakli and W. A. van Hook, J. Phys. Chem. **85**, 3480 (1981).
[24] H. Tanaka, H. Touhara, K. Nakanishi, and N. Watanabe, J. Chem. Phys. **80**, 5170 (1984).
[25] H. Tanaka, K. Nakanishi, and H. Touhara, J. Chem. Phys. **82**, 5184 (1985).
[26] R. A. Kuharski and P. J. Rossky, J. Am. Chem. Soc. **106**, 5786 (1984).
[27] R. A. Kuharski and P. J. Rossky, J. Am. Chem. Soc. **106**, 5794 (1984).
[28] P. Cristinziano, F. Lelj, P. Amodeo, and V. Barone, Chem. Phys. Lett. **140**, 401 (1987).
[29] E. S. Boek and W. J. Briels, J. Chem. Phys. **98**, 1422 (1993).
[30] J. Hernández-Cobos, I. Ortega-Blake, M. Bonilla-Marin, and M. Moreno-Bello, J. Chem. Phys. **99**, 9122 (1993).
[31] P.-O. Åstrand, A. Wallqvist, G. Karlström, and P. Linse, J. Chem. Phys. **95**, 8419 (1991).
[32] P.-O. Åstrand, A. Wallqvist, and G. Karlström, J. Phys. Chem. **98**, 8224 (1994).
[33] J. Pranata, J. Phys. Chem. **99**, 4855 (1995).
[34] A. D. Buckingham, *Intermolecular Interactions: From Diatomics to Biopolymers* (Wiley, New York, 1978).
[35] M. Levitt, M. Hirshberg, R. Sharon, and V. Daggett, Comp. Phys. Commun. **91**, 215 (1995).
[36] M. Levitt, J. Mol. Biol. **168**, 595 (1983).
[37] M. Levitt and R. Sharon, Proc. Natl. Acad. Sci. USA **85**, 7557 (1988).
[38] V. Daggett and M. Levitt, Chem. Phys. **158**, 510 (1991).
[39] K. Kirshenbaum and V. Daggett, Biochemistry **34**, 7629 (1995).
[40] K. E. Laidig and V. Daggett, J. Phys. Chem. **100**, 5616 (1996).
[41] M. Levitt, M. Hirshberg, R. Sharon, and V. Daggett (in preparation).
[42] P.-O. Åstrand, A. Wallqvist, and G. Karlström, J. Chem. Phys. **100**, 1262 (1994).
[43] R. J. Meier and B. Coussens, J. Mol. Struct. **253**, 25 (1992).
[44] A. Johansson, P. Kollman, S. Rothenberg, and J. McKelvey, J. Am. Chem. Soc. **96**, 3794 (1974).
[45] G. Algona, A. Pullman, E. Scroco, and J. Tomusi, Int. J. Peptide Protein Res. **5**, 251 (1973).
[46] X.-C. Wang, J. C. Facelli, and J. Simons, Int. J. Quantum Chem. **45**, 123 (1993).
[47] H. J. Christoffers and G. Kegeles, J. Am. Chem. Soc. **85**, 2562 (1963).
[48] A. V. Wolf, M. G. Brown, and P. G. Prentiss, *CRC Handbook of Chemistry and Physics*, edited by R. C. Weast (Chemical Rubber, Boca Raton, 1984–1985), Vol. 65, p. D222.
[49] Y. Harpaz, M. Gerstein, and C. Chothia, Structure **2**, 641 (1994).
[50] L. E. Chirlian and M. M. Francl, J. Comput. Chem. **8**, 894 (1987).
[51] C. M. Breneman and K. B. Wiberg, J. Comput. Chem. **11**, 361 (1990).
[52] P. C. Harihan and J. A. Pople, Theor. Chem. Acta **28**, 213 (1973).
[53] M. P. Allen and D. J. Tildesley, *Computer Simulation of Liquids* (Oxford University, Oxford, 1993).
[54] F. Franks, *Water* (The Royal Society of Chemistry, London, 1983).
[55] M. Gerstein, J. Tsai, and M. Levitt, J. Mol. Biol. **249**, 955 (1995).
[56] L. Andrussow and B. Schramm, *Landolt–Börnstein*, edited by K. Schäfer (Springer, Berlin, 1969), Vol. 5, Bandteil a, p. 639.
[57] J. L. Finney and J. Turner, Electrochim. Acta **33**, 1183 (1988).
[58] C. Chipot, C. Millot, B. Magret, and P. A. Kollman, J. Chem. Phys. **101**, 7953 (1994).
[59] C. A. Swensen, Arch. Biochem. Biophys. **117**, 494 (1966).
[60] P. R. Philip, G. Perron, and J. E. Desnoyers, Can. J. Chem. **52**, 1709 (1974).
[61] J. R. Reimers and M. L. Klein, Chem. Phys. **64**, 95 (1982).
[62] L. J. Gosting and D. F. Akeley, J. Am. Chem. Soc. **74**, 2058 (1952).
[63] J. G. Albright and R. Mills, J. Phys. Chem. **69**, 3120 (1965).
[64] J. L. Finney and J. Turner, Ann. NY Acad. Sci. **482**, 127 (1986).